Compact strain-sensitive flexible photonic crystals for sensors

Otto L. J. Pursiainen[a] and Jeremy J. Baumberg
School of Physics and Astronomy, University of Southampton, SO17 1BJ, Southampton, United Kingdom

Kevin Ryan
Merck Chemicals, University Parkway, Chilworth, SO16 7QD, Southampton, United Kingdom

Josef Bauer and Holger Winkler
Merck KGaA, Frankfurter Strasse 250, D-64291 Darmstadt, Germany

Benjamin Viel and Tilmann Ruhl
Deutsches Kunststoff-Institut (DKI), Schlossgartenstrasse 6, D-64289 Darmstadt, Germany

(Received 7 April 2005; accepted 5 July 2005; published online 30 August 2005)

A promising fabrication route to produce absorbing flexible photonic crystals is presented, which exploits self-assembly during the shear processing of multi-shelled polymer spheres. When absorbing material is incorporated in the interstitial space surrounding high-refractive-index spheres, a dramatic enhancement in the transmission edge on the short-wavelength side of the band gap is observed. This effect originates from the shifting optical field spatial distribution as the incident wavelength is tuned around the band gap, and results in a contrast up to 100 times better than similar but nonabsorbing photonic crystals. An order-of-magnitude improvement in strain sensitivity is shown, suggesting the use of these thin films in photonic sensors. © *2005 American Institute of Physics*. [DOI: 10.1063/1.2032590]

Synthesis of three-dimensional (3D) photonic crystals based on synthetic opals has been well developed over the past decade,[1–3] with a particular focus on in-filling with high-refractive-index media to create true 3D band gaps.[1,4] However, the application of 3D photonic crystals has been restricted compared to the advanced technology built on two-dimensional photonic crystals fabricated from patterned planar waveguides.[5–7] Here we present an alternative approach to fabricating useful photonic crystals based on the extrusion self-assembly of low-contrast flexible photonic nanomaterials. Tuning of the band gaps with angle and strain is clearly observed in these films. However, as is typical in polymer-based photonic crystals, the dielectric nanostructures exhibit a low on/off contrast at the edges of the Bragg scattering peaks making their incorporation into sensors problematic. We show that by introducing an absorbing material into the surroundings of the polymer spheres (which is very easy to achieve in this process), the transmission contrast can be increased by a factor of >100, leading to prospective applications in compact vibration and thermal sensors. We analyze this behavior in terms of the optical field distribution on either side of the band gap, and show that absorbing 3D photonic crystals inherently improve on the performance of absorbing one-dimensional (1D) photonic crystals (Bragg mirrors).

Our sample precursors consist of hard polystyrene (PS) cores, covered by a poly(methylmethacrylate) (PMMA) interlayer, and a polyethylacrylate (PEA) shell. Self-assembly processes occur during the shearing by uniaxial compression of the precursor melt resulting in fcc crystallization of the PS-PMMA cores, with the soft PEA shell material filling the spaces between the PS-PMMA lattice sites thus forming an elastic film. Hence the (111) plane of the fcc lattice is parallel to the sample surface. A detailed description of the precursors and the manufacturing is reported elsewhere.[8] The final samples used here are disks with a diameter of 10 cm and a thickness of around 250 μm [Fig. 1(a)].

Angle-dependent reflection measurements were carried out to identify the final lattice pitch and average refractive index. Monochromatic light was collimated and focused on the sample surface, and the reflection spectra recorded for incident angles of 20–60° [Fig. 1(c)]. The shift in the peak wavelength can be modeled using standard Bragg diffraction

$$4d_{111}^2(\bar{n}^2 - \sin^2\theta) = \lambda_{111}^2, \tag{1}$$

where d_{111} is the (111)-fcc-plane spacing, $\bar{n}$ the effective refractive index, θ the angle of incidence, and λ_{111} the wave-

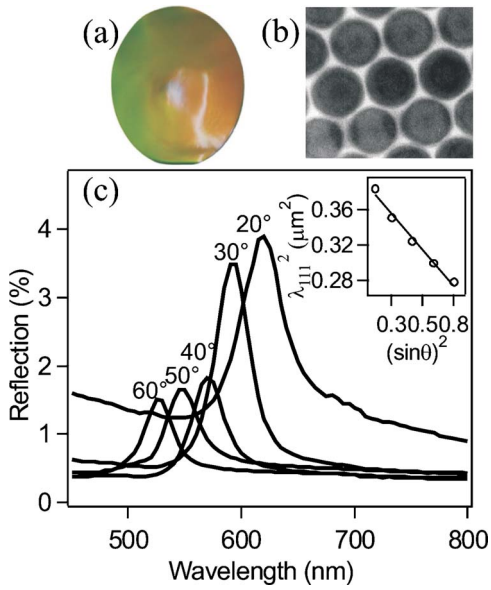

FIG. 1. (Color online) (a) Optical and (b) TEM image of the sample (111) surface. (c) Angle-dependent reflection spectra of the αPX sample. Inset: Peak position vs angle.

[a]Author to whom correspondence should be addressed; electronic mail: otto@phys.soton.ac.uk

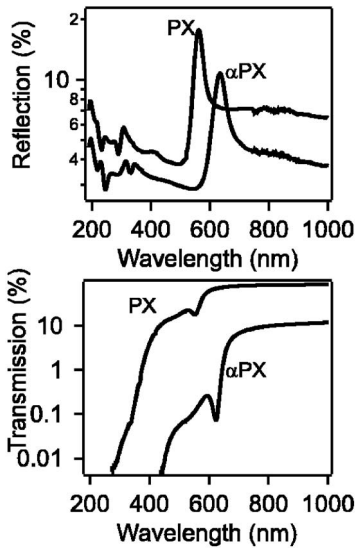

FIG. 2. Reflection and transmission spectra of an absorbing (αPX) and a nonabsorbing (PX) photonic crystal.

length of the Bragg peak. The changing location of the Bragg peak wavelength is clearly visible due to the θ dependence of the resonance. By plotting [Fig. 1(c), inset] λ_{111}^2 against $\sin^2\theta$ (assuming constant refractive index) we extract $d_{111}=202$ nm and an effective refractive index of 1.56. The 3 dB bandwidth of the diffraction peaks in Fig. 1(c) remains approximately constant around 35 nm. The agreement with the expected plane spacing from transmission electron microscopy (TEM) images of the sample surfaces [Fig. 1(b)], which also show the high degree of ordering and the hexagonal symmetry of the surface (111) plane, confirms the good organization of these photonic crystals.

The transmission and reflection spectra at normal incidence of an absorbing photonic crystal (αPX) and a nonabsorbing photonic crystal (PX) were measured using a spectrophotometer (Fig. 2). In this case, the absorption is introduced by distributing 0.2 wt % of carbon black into the pre-extrusion mix, providing a spectrally featureless attenuation. While the transmission drop across the band gap is not at all pronounced for the nonabsorbing PX sample, a drop of over two orders of magnitude in the transmission is readily observed in the αPX sample. Similar results are found for other samples of different periodicity, confirming that this result is not due to spectral features in the absorbing component. The reflection peak at the 1st Bragg resonance (around 634 nm αPX, and 560 nm PX) is unaffected by this absorption process. The second Bragg peak, visible at 315 nm (270 nm) for the αPX (PX), is also only weakly affected. Thus while absorption has a profound effect on transmission, it has a relatively weak effect on reflection. Hence we consider here device applications in transmission mode.

The asymmetric transmission spectral shape across the band gap is produced because of the different optical field distributions for wavelengths on either side of the band gap. The volume between the polystyrene spheres has a lower refractive index, and thus supports the optical mode with a shorter wavelength.[9] Since this interstitial region contains most of the absorber, the short wavelength modes experience considerably higher absorption than the long wavelength modes on the other side of the band gap. The situation is thus different from the case considered by Biswas *et al.*,[10] where the absorption takes places in the material with higher refractive index. To confirm this, we model the reflection and transmission through such absorbing periodic structures of different dimensionality. We rewrite the absorption coefficient per unit cell, $\alpha=\alpha_0\bar{f}(1+\chi)$, in terms of an enhancement factor, χ, the absorption coefficient of the low-refractive-index material, α_0, and the volume filling fraction of the interstitial absorbing material, $\bar{f}$, which is 26% in a close-packed fcc lattice. Assuming small band gaps which is true for the weak refractive contrast $\Delta n/\bar{n}$ here, the enhancement can then be shown to be

$$\chi=\frac{\Delta\omega/\bar{\omega}}{\bar{f}\Delta n/\bar{n}}, \tag{2}$$

where $\bar{\omega}$ is the Bragg frequency, $\bar{n}$ is the volume averaged refractive index, and $\Delta\omega$ is the band gap width. The ratio of the modified transmission below and above the band gap can then be estimated as

$$T_{\min}/T_{\max}=\bar{T}^{\chi}, \tag{3}$$

where $\bar{T}$ is the transmission without the PX resonance enhancement. In 3D fcc-photonic crystals, our calculations show that χ can exceed 4, which with the averaged transmission $\bar{T}$ of around 10% gives a transmission contrast ratio of 10^{-4}. This should be compared with similar estimates for 1D multilayers which have a fill fraction of only 50% and confine the field less effectively in the different layers on either side of the band gap, leading to a maximum $\chi\sim 1.5$. Hence the 3D αPX scenario is three orders of magnitude more effective than the 1D weak absorptive Bragg grating (for instance, as used for fiber sensors). In addition, the observed abrupt transmission edge requires only sub-mm device lengths and our straightforward manufacturing process should be compared to other less scalable techniques devised for colloidal crystals.[1–3] Our experimental results do not fully reach the predicted contrast, most likely due to the interplay of the full set of 16 standing wave modes that exist in the vicinity of the first zone-center photonic band gap seen along the [111] direction,[11] or due to the inhomogeneous distribution of absorbing material around the PS cores. Further modeling of 3D photonic crystals rigorously incorporating absorption is currently in progress to confirm the details of this mechanism. However, our basic model confirms that the sharp transmission contrast is brought about by the interplay of the band gap and the absorptive material in the low-refractive-index component.

In order to evaluate the properties of the flexible absorptive photonic crystals for sensor applications, we measure their reflection and transmission properties as a function of strain. A 1-cm-wide strip of αPX film was uniformly stretched with a micrometer-controlled sample holder while the optical properties were measured *in situ* (Fig. 3). The shifting of the (111) plane band gap is clearly visible in both transmission and reflection spectra, as the strain is increased from 0% to 2%, 4%, 8%, and 13%. The plummeting transmission edge retains its steep slope throughout this range of strains, while the minimum transmission dip also shifts and increases only slightly. The reflection spectra show an identical shift of the (111)-plane Bragg-peak towards shorter wavelengths, reaching a −5% wavelength shift at the maximum +13% strain. The shifting peak wavelength clearly cor-

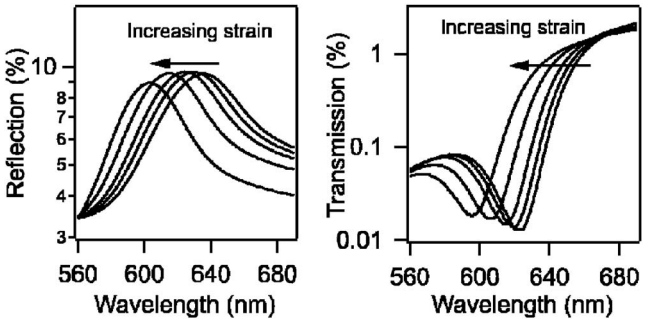

FIG. 3. Strain-induced shifts in reflection (left) and transmission (right) of the absorbing photonic crystal, as the strain is increased from 0% to 2%, 4%, 8%, and 13%.

responds to a contraction in the (111)-plane separation. Fitting the dependence of the contraction in thickness with the strain along the film allows the Poisson ratio, $\sigma \sim 0.4$, to be determined, comparable to similar elastomers.[12] Although strained photonic crystals have been measured before,[13–15] this is the first time to our knowledge that such a measurement has been carried out on an ordered composite material composed of hard spheres in an elastic absorbing matrix.

The steep shifting transmission edge is a very attractive property from an applications point of view. To characterize this we define a sensitivity S which is given by the fractional change in transmission per 1% increase in strain. Figure 4 shows this sensitivity for a nonabsorbing (PX) and absorbing (αPX) photonic crystal. The absorbing flexible photonic

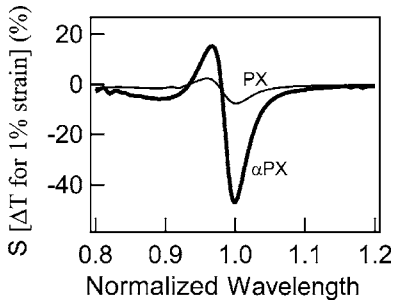

FIG. 4. Strain sensitivity of the absorbing (αPX) and nonabsorbing (PX) photonic crystals, defined as the fractional transmission change produced by a 1% increase in strain. The wavelength is normalized to the Bragg peak.

crystal has almost ten times the sensitivity of the nonabsorbing crystal, reaching nearly 50% transmission reduction for only 1% strain. We note that this improvement is not at the cost of either operational spectral bandwidth or maximum strain.

In conclusion, we show that a new fabrication route to 3D photonic crystals exploiting the self-assembly during extrusion of polymeric spheres can produce flexible photonic materials. By incorporating an absorbing component in the low-refractive-index interstitial voids of the fcc lattice, the transmission shows a very steep roll-off on the short-wavelength side of the photonic band gap. We account for this in terms of a simple model of the optical field distributions, and show how it can be utilized in improved sensors. We note that these ideas can be further exploited by using resonant absorbing and refractive materials tuned around the band gap, such as metal nanoparticles, semiconductor quantum dots and organic semiconductors.

This work was supported by the EPSRC-GB Portfolio Partnership EP/C511786/1, and by Merck KGaA.

[1] P. Ni, P. Dong, B. Cheng, X. Li, and D. Chang, Adv. Mater. (Weinheim, Ger.) **13**, 437 (2001).
[2] P. T. Miclea, A. S. Susha, Z. Liang, F. Caruso, C. M. Sotomayor Torres, and S. G. Romanov, Appl. Phys. Lett. **84**, 3960 (2004).
[3] G. Subramania, K. Constant, R. Biswas, M. M. Sigalas, and K.-M. Ho, Appl. Phys. Lett. **74**, 3933 (1999).
[4] J. E. G. J. Wijnhoven and W. L. Vos, Science **281**, 802 (1998).
[5] R. T. Neal, M. Zoorob, M. D. Charlton, G. J. Parker, C. E. Finlayson, and J. J. Baumberg, Appl. Phys. Lett. **84**, 2415 (2004).
[6] A. Chutinan and S. John, Phys. Rev. E **71**, 026605 (2005).
[7] M. V. Kotlyar, T. Karle, M. D. Settle, L. O'Faolain, and T. F. Krauss, Appl. Phys. Lett. **84**, 3588 (2004).
[8] T. Ruhl, P. Spahn, and G. P. Hellmann, Polymer **44**, 7625 (2003).
[9] J. D. Joannopoulos, R. D. Meade, and J. N. Winn, *Photonic Crystals — Molding the Flow of Light* (Princeton University Press, Princeton, NJ, 1995).
[10] R. Biswas, M. M. Sigalas, G. Subramania, and K.-M. Kelo, Phys. Rev. B **57**, 3701 (1998).
[11] F. Lopez-Tereira, T. Ochiai, K. Sakoda, and J. Sanchez-Dehesa, Phys. Rev. B **65**, 195110 (2002).
[12] L. E. Nielsen, *Mechanical Properties of Polymers* (Reinhold, New York, 1967).
[13] K. Busch and S. John, Phys. Rev. E **58**, 3896 (1998).
[14] J. M. Jethmalani and W. T. Ford, Chem. Mater. **8**, 2138 (1996).
[15] S. H. Foulger, P. Jiang, Y. Ying, A. C. Lattam, D. W. Smith, Jr., and J. Ballato, Langmuir **17**, 6023 (2001).